

## Synthesis, Structural and spectral investigations of Co<sup>2+</sup> doped Cadmiumborate nanocomposite

P.N.V.V.L. Pramila Rani<sup>1</sup>, D.Ramachandran<sup>1</sup>, R.V.S.S.N. Ravi Kumar<sup>2</sup>.

*Dept. of Chemistry, Acharya Nagarjuna University, Nagarjuna Nagar, Guntur, AP*

*Dept. of Physics, Acharya Nagarjuna University, Nagarjuna Nagar, Guntur, AP*

*Corresponding Author: P.N.V.V.L. Pramila Rani*

**Abstract:** Co<sup>2+</sup> doped Cadmiumborate nanocomposite (Co<sup>2+</sup> doped Cd<sub>3</sub>(BO<sub>3</sub>)<sub>2</sub> NC) was synthesized at room temperature by chemical precipitation method. The prepared Co<sup>2+</sup> doped Cd<sub>3</sub>(BO<sub>3</sub>)<sub>2</sub> NC is characterized by X-ray diffraction (X-RD), Scanning Electron Microscopy (SEM) /EDS, Electron paramagnetic resonance (EPR), Optical studies, Photoluminescence studies and Fourier transform infrared (FT-IR) techniques. From XRD structure and size of the crystallites are evaluated by using Scherrer's formula. SEM images show the stone like morphology of nanocomposite. Optical absorption spectrum indicates the distorted octahedral site symmetry of Co<sup>2+</sup> ions. The crystal field Dq and interelectronic repulsion parameters B and C are evaluated. PL spectra indicate clearly that the doping of Co<sup>2+</sup> in the host matrix lead to significant changes in PL intensity. EPR spectrum gives resonance lines at g<sub>1</sub> = 2.00 and g<sub>⊥</sub> = 2.08 for Co<sup>2+</sup> doped ions. FT-IR spectrum reveals the characteristic vibrations of Cadmium borate. Thus this nanocomposite can exhibit an optoelectronic properties and technological importance in the development of tunable solid state lasers and new luminescent materials.

**Key words:** Co<sup>2+</sup> doped Cadmiumborate nanocomposite, Synthesis, structure, SEM/EDX, EPR, Optical, photoluminescence,

Date of Submission: 14-12-2018

Date of acceptance: 29-12-2018

### I. INTRODUCTION

Semiconductor nano particles have attracted much attention due to different physical and chemical properties compared to their bulk materials. Dilute magnetic semiconductors (DMSs) in which some of the cations host lattice are replaced by a transition metal ions have attracted considerable attention due to their potential as spin-polarized carrier sources and their potential applications in spintronic devices [1-5]. The continuous attempts to develop next generation devices equipped with multi functions are now being extended to the search for materials that can combine magnetic, electronic, and photonic responses. One example of such efforts is the quest for a ferromagnetic material that can inject spin polarized carriers into semiconductors [6].

In recent years, interest in borates containing metal ions has grown because they have properties of technological importance in electronics, tunable and fiber optic communication systems[7,8]. These novel physical and chemical properties which are essential for nano electronics [9], biological [10], and catalytic applications. These applications drive scientific community to probe its electronic structure through exciton dynamics. Boron-based compounds are promising systems due to their high temperature thermoelectric properties [11].

Metallic cobalt nanoparticles have been available from wet-phase synthesis methods for more than 50 years, today offering good control of product size and shape. Cobalt nano particles possess magnetic properties, which leads to applications in imaging, sensors and many other areas [12]. The enhanced mechanical, electronic and magnetic properties [13] of metallic nano particles have triggered proposals for applications as high-density magnetic storage devices [14], hall sensors [15], soft magnetic materials exhibiting higher permeability/lower coercivity [16] and heterogeneous catalysts [17]. Transition metallic (Fe, Co, Ni) nano particles have found wide application in catalysts, solar energy absorption and magnetic recording [8-20]. Applications for cobalt nano nanocomposite generally involve their magnetic properties and include catalysts and magnetic recording and in medical sensors and bio medicine as a contrast enhancement agent for magnetic resonance imaging. Cobalt nano powders are also being tested for site specific drug delivery agents for cancer therapies and in coatings, fuel cells, batteries, DNA circuits and chrome replacement in sporting goods, luxury and consumer products [21].

Chemical precipitation method is one of the most popular techniques that are used in industrial applications because of the cheap raw materials, easy handling and large-scale production [22].

## II. RESULTS AND DISCUSSION

### 2.1. Powder X-ray diffraction study

The synthesized  $\text{Co}^{2+}$  doped Cadmiumborate NC showed in Fig.1.

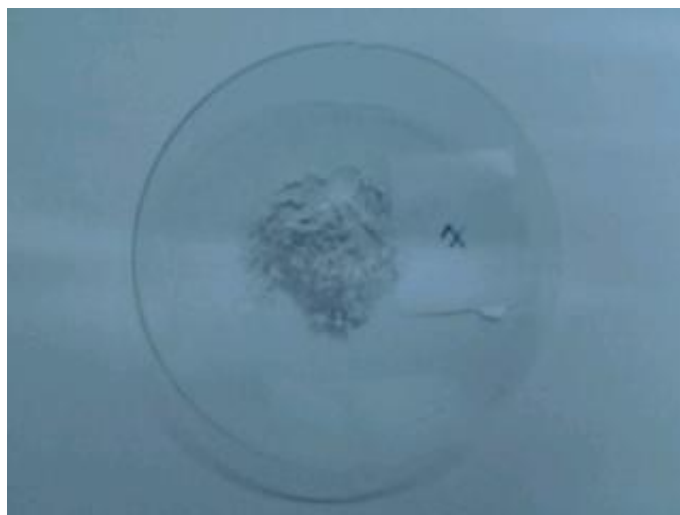


Fig.1  $\text{Co}^{2+}$  doped cadmiumborate nanocomposite

In this work the cadmium borate phase formation condition has been investigated by XRD. Fig.2 shows the powder X-ray diffraction patterns of  $\text{Co}^{2+}$  doped  $\text{Cd}_3(\text{BO}_3)_2$  nanocomposite. The characteristic diffraction peaks of orthorhombic crystal structure of cadmium borate are noticed in  $\text{Co}^{2+}$  doped  $\text{Cd}_3(\text{BO}_3)_2$  NC and the corresponding lattice cell parameters are evaluated [23].

$$a = 0.598, b = 0.476, c = 0.905 \text{ nm and } V = 25.801 \text{ nm}^3$$

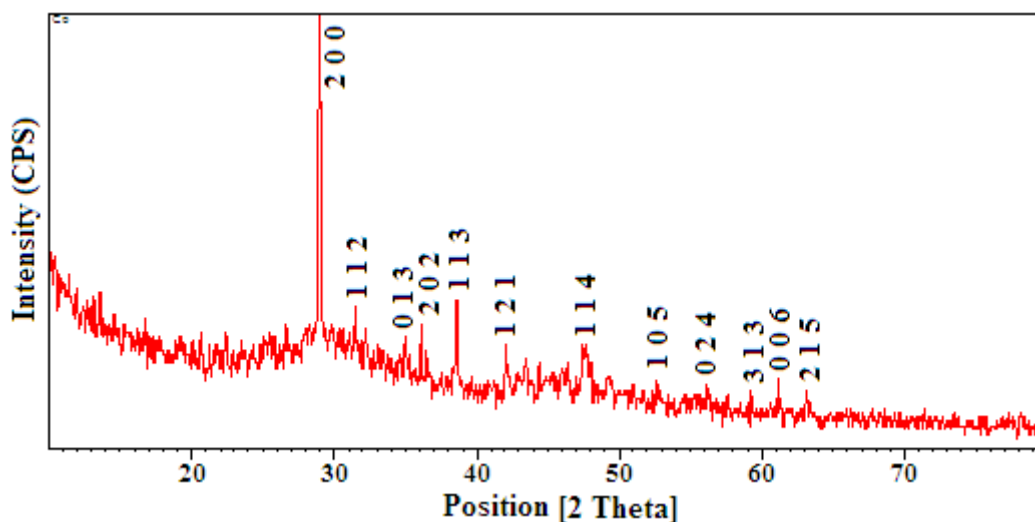


Fig.2. X-RD of  $\text{Co}^{2+}$  doped cadmiumborate nanocomposite

The average crystallite size of the particle according to Scherrer's equation,  $D = 0.9\lambda / \beta \cos\theta$ , where D is crystallite size (nm),  $\lambda$  is X-ray wavelength,  $\beta$  is full width at half maximum intensity and  $\theta$  is diffraction angle. The evaluated average crystallite size is 42 nm for  $\text{Co}^{2+}$  doped sample.

### 3.2 SEM and EDS study

The morphology and microstructure of prepared nanocomposite(NC) was investigated using SEM. The morphological images of as prepared cadmium borate NC sample is given in Fig.3. SEM images of  $\text{Co}^{2+}$  ion exhibits the irregular particle like surface morphology. Heat treatment resulted in agglomeration of the NC (nanocomposite) as a function of temperature. Therefore, some degree of agglomeration at the higher calcination temperature appears unavoidable. In many cases of nano-crystalline materials, it was observed that a tendency of agglomeration among the nanoparticles [24].

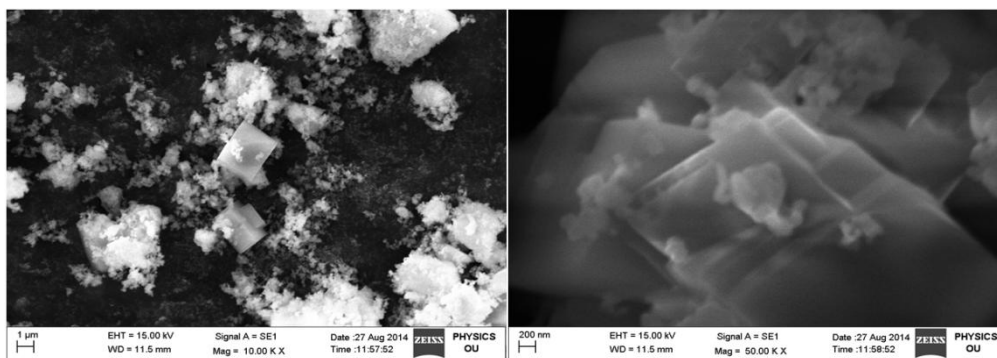


Fig.3 SEM images of  $\text{Co}^{2+}$  doped cadmiumborate nanocomposite

The elemental composition analysis of  $\text{Co}^{2+}$  doped  $\text{Cd}_3(\text{BO}_3)_2\text{NC}$  specimens was carried out using EDS. Fig.4 shows EDS pattern of  $\text{Co}^{2+}$  doped  $\text{Cd}_3(\text{BO}_3)_2\text{NC}$ . The EDS spectrum gives the information about chemical composition of the elements present from surface to interior of the solids and to confirm the homogeneity of the investigated samples. The EDS data indicate the distribution of Cd, Co and oxygen species along with chemical composition mapping. This clearly indicates the presence of metal ions.

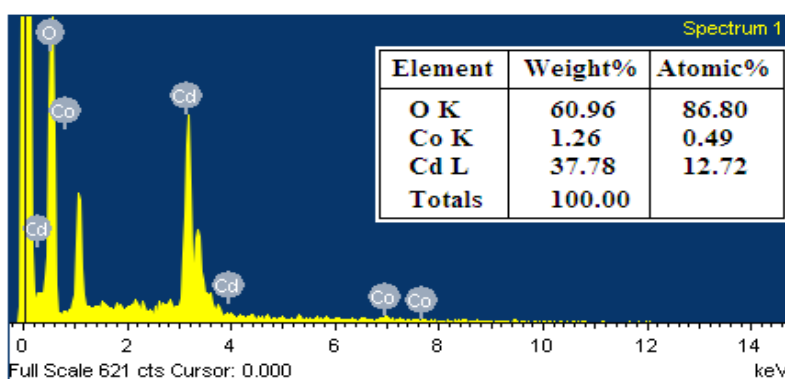


Fig.4. EDS of  $\text{Co}^{2+}$  doped cadmiumborate nanocomposite

### 3.3 Optical Absorption Study

Optical absorption spectrum of  $\text{Co}^{2+}$  doped  $\text{Cd}_3(\text{BO}_3)_2\text{NC}$  was shown in Fig.5. The optical absorption spectrum exhibits absorption bands at 447, 478, 561, 657 and 1203 nm. Accordingly three spin allowed transitions  ${}^4\text{T}_{1g}(\text{F}) \rightarrow {}^4\text{T}_{2g}(\text{F})$ ,  ${}^4\text{T}_{1g}(\text{F}) \rightarrow {}^4\text{A}_{2g}(\text{F})$  and  ${}^4\text{T}_{1g}(\text{F}) \rightarrow {}^4\text{T}_{1g}(\text{P})$  are to be expected. Out of these  ${}^4\text{T}_{1g}(\text{F}) \rightarrow {}^4\text{A}_{2g}(\text{F})$  involves a double electron jump ( $t_{2g}^2 e_g^2 \rightarrow t_{2g}^3 e_g^4$ ) and is therefore expected to be weak [25]. The two bands observed in the present investigation at 1206 and 561 nm are attributed to two spin allowed transitions from ground state  ${}^4\text{T}_{1g}(\text{F})$  to excited states  ${}^4\text{T}_{2g}(\text{F})$  and  ${}^4\text{A}_{2g}(\text{F})$  respectively. Accordingly the other three bands are attributed to transitions  ${}^4\text{T}_{1g}(\text{F}) \rightarrow {}^2\text{A}_{1g}(\text{G})$ ,  ${}^4\text{T}_{1g}(\text{P})$  and  ${}^2\text{T}_{1g}(\text{G})$  respectively. In  $\text{O}_h$  symmetry theoretically the ratios of energies of transitions  ${}^4\text{T}_{1g}(\text{F}) \rightarrow {}^4\text{A}_{2g}(\text{F})$ :  $\nu_2$  and  ${}^4\text{T}_{1g}(\text{F}) \rightarrow {}^4\text{T}_{2g}(\text{F})$ :  $\nu_1$  are almost invariable from 1.9 to 2.2 [26]. In the present case from the band positions the ratio of  $\nu_2$  to  $\nu_1$  is 2.1 [27].

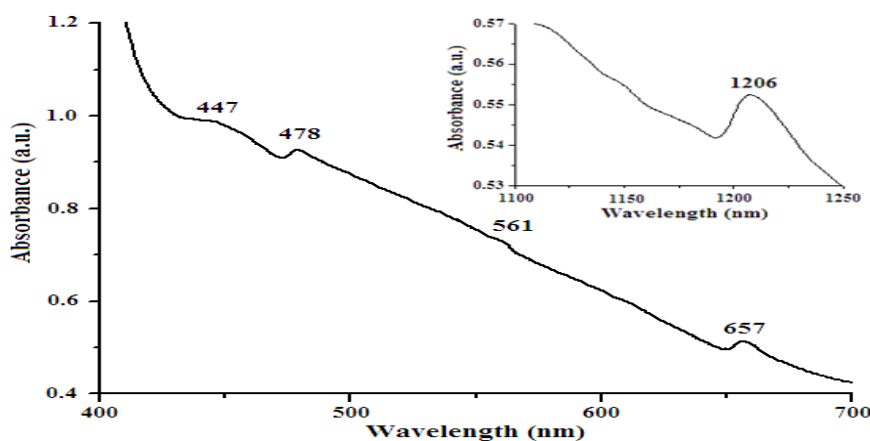


Fig.5. Optical of  $\text{Co}^{2+}$  doped cadmiumborate nanocomposite

The energy matrix for (d<sup>7</sup>) configuration is solved for different sets of crystal field (Dq) and inter-electronic repulsion (B and C) parameters. These parameters give good fit with the observed band positions at Dq = 950, B = 920, C = 3450 cm<sup>-1</sup>. The free ion value of B for Co<sup>2+</sup> is 1120 cm<sup>-1</sup> [28]. The reduction of 25% of free ion of B indicates moderate covalent. The band attributed to the transition <sup>4</sup>T<sub>1g</sub>(F) → <sup>4</sup>T<sub>2g</sub>(F) is broad and its observed value 1206 nm shows considerable deviation from the calculated value. These features might be due to distortion from octahedral symmetry of Co<sup>2+</sup> site in the material. The observed band head data and the calculated values are given in Table 1.

**Table 1** Observed and calculated band positions for Co<sup>2+</sup> doped Cd<sub>3</sub>(BO<sub>3</sub>)<sub>2</sub> nanocomposite

Transition From <sup>4</sup> T <sub>1g</sub> (F)	Observed band position		Calculated Wavenumber (cm <sup>-1</sup> )
	Wavelength (nm)	Wavenumber (cm <sup>-1</sup> )	
<sup>4</sup> T <sub>2g</sub> (F)	1206	8314	8314
<sup>2</sup> T <sub>1g</sub> (G)	657	15220	15195
<sup>4</sup> A <sub>2g</sub> (F)	561	17825	17814
<sup>4</sup> T <sub>1g</sub> (P)	478	20920	20928
<sup>2</sup> A <sub>1g</sub> (G)	447	22371	22344

### 3.4 EPR Study

The EPR spectrum of Co<sup>2+</sup> doped Cd<sub>3</sub>(BO<sub>3</sub>)<sub>2</sub> nanocomposite was observed only at low temperatures because the spin lattice relaxation time is extremely short for octahedral coordination of Co<sup>2+</sup> [29-31] ions at low spin and spectrum of sample present in Fig.6. There are eight line hyperfine splitting of spectrum was observed at frequency 9.17965 GHz.

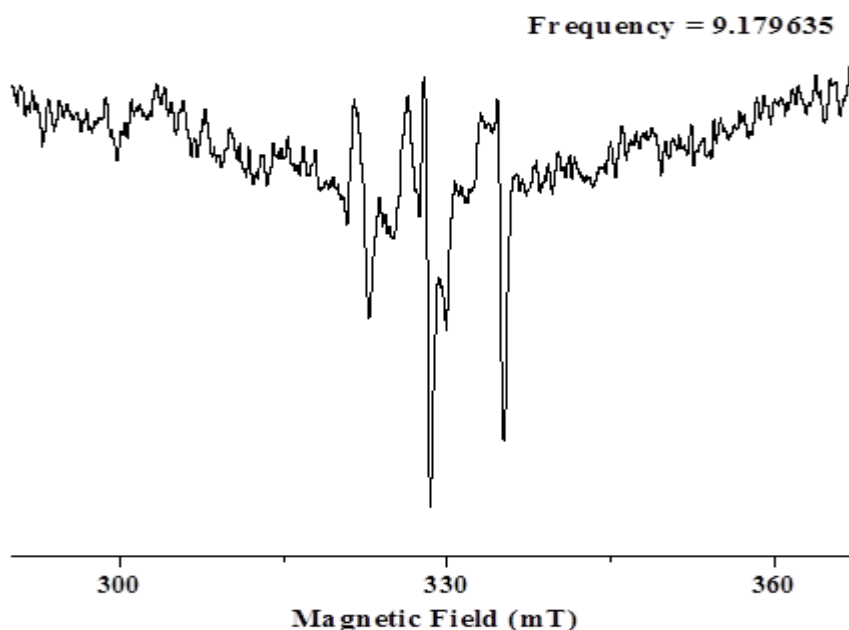


**Fig.6.** EPR of Co<sup>2+</sup> doped cadmiumborate nanocomposite

In the present investigation, EPR spectrum of Co<sup>2+</sup> doped Cd<sub>3</sub>(BO<sub>3</sub>)<sub>2</sub> NC sample exhibit resonance lines at g<sub>||</sub> = 2.00 and g<sub>⊥</sub> = 2.08 [32] at 5 K temperature. By correlating EPR and optical absorption spectral data, the parameter of covalency (k<sub>0</sub>) has been evaluated by the relation [33].

$$g = (10/3) + k_0 - (15/2) (\lambda/\Delta)$$

where g is the observed g-factor, 'λ' is the spin-orbit coupling constant (-178 cm<sup>-1</sup> for Co<sup>2+</sup>) and Δ is the energy of transition from <sup>4</sup>T<sub>1g</sub>(F) → <sup>4</sup>T<sub>2g</sub>(F). The value of k<sub>0</sub> lies between 0.5 and 1.0, the limits of pure covalent and pure ionic bonding, respectively. In the present investigation, the calculated value of k<sub>0</sub> is 0.83 indicating the bonding between the Co<sup>2+</sup> and the ligands to be partially covalent.

### 3.5 Photoluminescence Study

For the optical properties of nanoparticles surface states are very important for the physical properties. In nanoparticles, most ions at the surface are non-saturated in coordination. Electrons and holes may be excited easily and escape from the ions. Many carriers trapped at the surface states or defect sites may be released by photo excitation [34,35]. So fluorescence efficiencies of nanocrystals are higher than those bulk materials. In order to study the role of doping induced defects on the PL behavior of synthesized cadmium borate NC emission was recorded at room temperature. Fig.7 depicts the emission spectrum of the Co<sup>2+</sup> doped Cd<sub>3</sub>(BO<sub>3</sub>)<sub>2</sub> NC under the photon excitation of 390 nm.

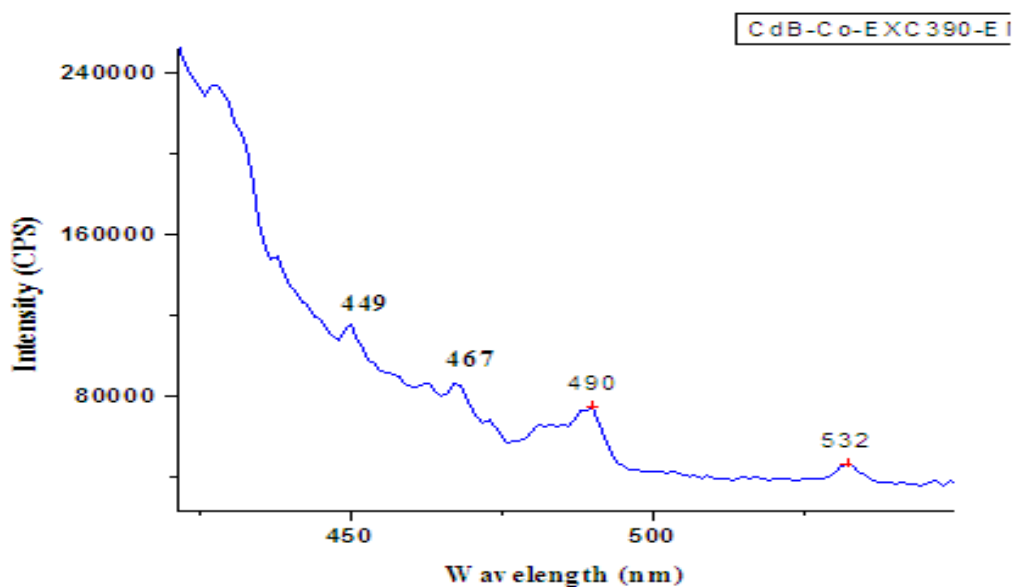


**Fig.7. PL of Co<sup>2+</sup> doped cadmiumborate nanocomposite**

Samples exhibit good UV emission band at 490, 532 nm and two relatively weak emission bands centered at 449 and 467 nm. The UV luminescence band belongs to the exciton recombination corresponding to near band edge (NBE) emission. UV emission centered weak band at 449 nm, weak blue emission centered at 467 nm and broad blue emission peak at 490 nm and another band at 532 nm with an excitation wavelength of 390 nm.

Co<sup>2+</sup> doped Cd<sub>3</sub>(BO<sub>3</sub>)<sub>2</sub>NC exhibited good UV blue-green emission. Crystal quality of synthesized NC can affect the origin and the intensity of UV emission and hence enhancement in UV emission is observed for the nanocomposite with better crystal quality. Therefore betterment in the crystal quality (less structural defects and impurities, such as oxygen vacancies and Cd interstitials) leads the sharp and strong origination of UV emission in the room temperature PL spectrum [36,37]. If the concentration of oxygen vacancies is reduced in the synthesized products then it results in the appearance of a sharp and strong intensity NBE emission [38].

### Chromatic Properties

The CIE 1931 chromaticity coordinates of Co<sup>2+</sup> doped Cd<sub>3</sub>(BO<sub>3</sub>)<sub>2</sub>NC was calculated from emission spectrum. The location of colour coordinates for Co<sup>2+</sup> doped Cd<sub>3</sub>(BO<sub>3</sub>)<sub>2</sub> NC in CIE chromaticity diagram is shown in Fig.8 by a solid circle (●). From this figure, one can see that the colour of Co<sup>2+</sup> doped Cd<sub>3</sub>(BO<sub>3</sub>)<sub>2</sub> NC located in whitish-blue region and the corresponding CIE coordinates are (x = 0.244, y = 0.196) and is useful for W-LEDs, electroluminescence panels and PDPs [39].

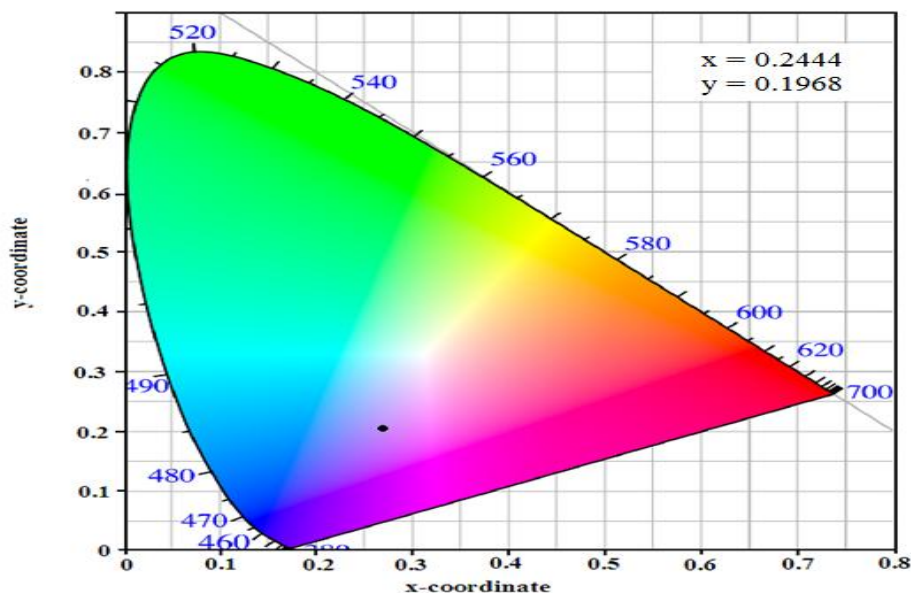


Fig.8. CIE of  $\text{Co}^{2+}$  doped cadmiumborate nanocomposite

### 3.6 FTIR:

FT-IR spectrum of  $\text{Co}^{2+}$  doped  $\text{Cd}_3(\text{BO}_3)_2$  NC exhibited the symmetric, asymmetric stretching and bending vibrations of water and hydroxyl groups of the compound. The FT-IR spectrum of  $\text{Co}^{2+}$  doped  $\text{Cd}_3(\text{BO}_3)_2$  NC is as shown in Fig.9.

In the higher energy region, the peak at  $3300\text{-}3500\text{ cm}^{-1}$  is assigned to O–H stretching gives rise to absorption in this region and the possibility of some adsorbed water [40]. The spectrum of  $\text{Co}^{2+}$  doped  $\text{Cd}_3(\text{BO}_3)_2$  NC can be divided into the following three regions,  $600\text{-}800\text{ cm}^{-1}$  is related to the bending vibrations of various borate arrangements of B–O–B,  $800\text{-}1000\text{ cm}^{-1}$  is taken as B–O stretching vibrations of tetrahedral  $\text{BO}_4$  and  $1200\text{-}1400\text{ cm}^{-1}$  correlated to B–O stretching vibrations of  $\text{BO}_3$  units. The band around  $1355\text{ cm}^{-1}$  is assigned to B–O stretching vibrations of trigonal  $(\text{BO}_3)^{3-}$  units in metaborates [41,42]. The band around  $690\text{ cm}^{-1}$  can be attributed to B–O–B bending vibration of bridges containing one trigonal and one tetrahedral boron. The peak around  $540\text{-}590\text{ cm}^{-1}$  can be attributed to the borate deformation modes such as in-plane bending of boron-oxygen triangles [43]. The observed IR band positions are given in Table.2

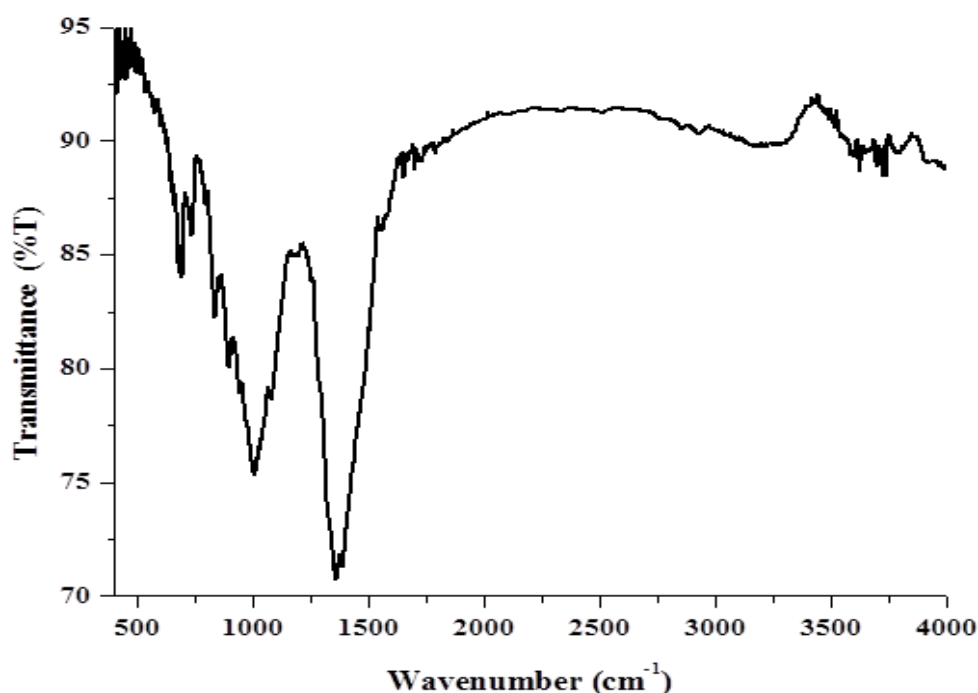


Fig.9. FT-IR spectrum of  $\text{Co}^{2+}$  doped  $\text{Cd}_3(\text{BO}_3)_2$  nanocomposite

**Table 2: Assignment of vibrational bands in FT-IR spectrum of Co<sup>2+</sup> doped Cd<sub>3</sub>(BO<sub>3</sub>)<sub>2</sub> nanocomposite**

Wavenumber (cm <sup>-1</sup> )	Assignment
1701	-OH Bending mode of vibration & change from BO <sub>3</sub> triangles to BO <sub>4</sub> tetrahedral
1355	Asymmetric stretching vibrations of borate triangles BO <sub>3</sub> and BO <sub>2</sub> O
1002	stretching vibrations of B-O linkages in BO <sub>4</sub> tetrahedral
690	B–O–B bending vibration of bridges containing one trigonal and one tetrahedral boron
552	Borate deformation modes such as the inplane bending boron-oxygen triangles

### III. CONCLUSIONS

In conclusion, chemical precipitation has been used successfully to produce Co<sup>2+</sup> doped Cd<sub>3</sub>(BO<sub>3</sub>)<sub>2</sub> NC.

- The crystal system is indexed to orthorhombic and lattice cell parameters are evaluated from the powder X-ray diffraction study. The average crystallite size for Co<sup>2+</sup> doped Cd<sub>3</sub>(BO<sub>3</sub>)<sub>2</sub> NC is 42 nm, indicates the formation of nanosized.
- SEM description shows the irregular shaped sphere like structures and EDS analysis confirms presence of ingredients of the prepared material.
- Optical absorption spectrum exhibited various bands and are assigned using T-S diagrams. The site symmetry of Co<sup>2+</sup> doped Cd<sub>3</sub>(BO<sub>3</sub>)<sub>2</sub> NC ascribed as octahedral for which crystal field (Dq) and inter-electronic repulsion (B, C) parameters are evaluated.
- EPR spectrum of Co<sup>2+</sup> doped Cd<sub>3</sub>(BO<sub>3</sub>)<sub>2</sub> NC sample exhibit resonance lines at  $g_{\parallel} = 2.00$  and  $g_{\perp} = 2.08$  at 100 K temperature. By correlating EPR and optical absorption data, the evaluated bonding parameter suggested that there exists a partially covalent bond between the doped Co<sup>2+</sup> ions and its ligands.
- PL spectrum exhibited UV emission band at 490, 532 nm and two relatively weak emission bands centered at 449 and 467 nm. After doping with copper ions, CIE coordinates are located in whitish-blue region and the corresponding CIE coordinates are (x = 0.2444, y = 0.1968).
- The vibrational modes of inorganic elements in prepared material was identified from FT-IR studies.

### ACKNOWLEDGMENTS

The Author P.N.V.V.L.Pramila Rani thankful for the financial support of UGC-BSR Meritorious Fellowship, (UGC-No.F.11-67/2008) to do my research work. Authors are thankful to the Director, Centralized Laboratory, Acharya Nagarjuna University for providing Ultracentrifuge.

### REFERENCES

- [1]. J.H.Shim, T.Hwang, S.Lee,J.H.Park and S.J.Han. "Origin of ferromagnetism in Fe and Cu-codoped ZnO", Applied Physics Letters, Vol.86,No.8, 2005, Article ID 082503.
- [2]. S. A. Wolf, D. D. Awschalom, R. A. Buhrman, J. M. Daughton, S. Von Molnar, M. L. Roukes, A. Y. Chichelkanova and D. M. Treger, "Spintronics: A Spin-Based Electronics Vision for the Future," Science, Vol. 294, No. 5546, 2001, pp. 1488-1495.
- [3]. S. Ghosh and K. Mandal, "Study of Zn<sub>1-x</sub>CoxO (0.02 < x < 0.08) Dilute Magnetic Semiconductor Prepared by Mechano synthesis Route," Journal of Magnetism and Magnetic Materials, Vol. 322, No. 14, 2010, pp. 1979-1984.
- [4]. H. Ohno, "Making Nonmagnetic Semiconductors Ferromagnetic,"Science, Vol. 281, No. 5379, 1998, pp. 951-956.
- [5]. G. A. Prinz, "Magneto-electronics," Science, Vol. 282, No.5394, 1998, pp. 1660-1663.
- [6]. G.Schmidt, D.Ferrand, L.W Molenkamp, A.T. Filip, B.J.V.Wees, Phys. Rev. B 62 (2002) R4790.
- [7]. W.D. Frago, C. de Mello Donega, R.L. Longo, J. Lumin. 105 (2003) 97.
- [8]. M. Muehlberg, M. Burianek, H. Edongue, J. Cryst. Growth 237 (2002) 740.
- [9]. O.Stier; M.Grundmann; D.Bimberg, Phys.Rev. B (1999), 59, 5688.
- [10]. A. Hosino; K. Fujioka; T. Oku; S.Nakamura; M. Suga;Y.Yamaguchi; K.Suzuki; M. Yasukara; K. Yamamoto, Microbiol. Immunol. (2004),48, 985.
- [11]. .Mori, J.Martin, G. Nolas, J. Appl. Phys., 102, (2007) 073510.

- [12]. G. N. Glavee, K. J. Klabunde, C. M. Sorensen, G. C. Hadjipanayis, "Sodium Borohydride Reduction of Cobalt Ions in Nonaqueous Media. Formation of ultrafine Particles (Nanoscale) of Cobalt Metal," *Inorganic Chemistry*, Vol. 32, No. 4, (1993), pp. 474-477.
- [13]. Q. Yan, T. Kim, A. Purkayastha, P. G. Ganesan, M. Shima and G. Ramanath, "Enhanced Chemical Ordering and Coercivity in FePt Alloy Nanoparticles by Sb-Doping," *Advanced Materials*, Vol. 17, (2005) 2233-2236.
- [14]. G. A. Held and G. Grinstein, "Quantum Limit of Magnetic Recording Density," *Applied Physics Letters*, Vol. 79,(2001) pp. 1501-1503.
- [15]. K. Tetz, L. Pang, and Y. Fainman, "High Resolution Surface Plasmon Resonance Sensor Based on Linewidth Optimized Nanohole Array Transmittance," *Optics Letters*, Vol. 31, (2006), pp. 1528-1530.
- [16]. B.H. Lee, Y. J. Lee, K. H. Min, D.-G. Kim and Y. D. Kim, "Synthesis of Nano Crystalline Spherical Cobalt- Iron (Co-Fe) Alloy," *Materials Letters*, Vol. 59, (2005) pp. 3156-3159.
- [17]. A. T. Bell, "The Impact of Nanoscience on Heterogeneous Catalysis" *Science*, Vol. 299, 2003, pp. 1688-1691.
- [18]. M. L. Wagner, L. D. Schmidt, Model Catalytic Oxidation Reactions: Oxygen with H<sub>2</sub>, NH<sub>3</sub>, and N<sub>2</sub>H<sub>4</sub>," *The Journal of Physical Chemistry*, Vol. 99, (1995) pp. 805-815.
- [19]. S. W. Moore, "Solar Absorber Selective Paint Research," *Solar Energy Materials*, Vol. 12, (1985) pp. 435-447.
- [20]. X. G. Li, A. Chiba and S. Takahashi, "Preparation and Magnetic Properties of Ultra Fine Particles of Fe—Ni Alloys," *Journal of Magnetism and Magnetic Materials*, Vol. 170, No. 3, (1997) pp. 339-345.
- [21]. E. Erb and A. M. El-Sherik, U.S. Patent, No. 5353266, 1994.
- [22]. A.H.Souici, N.Keghouche, J.A.Delaire, H.Remita, M.Mostafavi, "Radiolytic synthesis and optical properties of ultra-small stabilized ZnS nanoparticles". *Chem Phys Lett.* 422 (2006) 25–29.
- [23]. Y. Huazhao, M. Li, *Acta Crystallograp. E* 63 (2007) i50.
- [24]. J.K. Jakovljevic, M. Radoicic, T. Radetic, Z. Konstantinovic, Z.V. Saponjic, J. Nedeljkovic, *J. Phys. Chem. C* 113 (2009) 21029.
- [25]. S. Modak, M. Ammar, F. Mazaleyrat, S. Das, P.K. Chakrabarti, *J. Alloys Compd.* 473 (2009) 15.
- [26]. S. Koide, *Phil. Mag.* 4 (1959) 243.
- [27]. A.B.P. Lever, *Inorganic Electronic Spectroscopy*, 2<sup>nd</sup> Ed., Elsevier, Amsterdam (1984).
- [28]. Y. Tanabe, S. Sugano, *J. Phys. Soc. Jpn.* 9 (1959) 753.
- [29]. R.V.S.S.N. Ravikumar, A.V. Chandrasekhar, B.J. Reddy, Y.P. Reddy, J. Yamauchi, *Ferroelectrics* 274 (2002) 127.
- [30]. F. Gan, H. Deng, H. Liu, *J. Non-Cryst. Solids* 52 (1982) 143.
- [31]. E.A. Harris, *Phys. Chem. Glasses* 28 (1987) 196.
- [32]. A.C. Stephen, *Biochem. J.* 137 (1974) 587.
- [33]. W. Low, *Phys. Rev.* 109 (1957) 256.
- [34]. B.N. Figgis, *Introduction to Ligand Fields*, Wiley Eastern, New Delhi (1976).
- [35]. A. Geoffroy, E. Bringuier, *Appl. Phys. Lett.* 61 (1992) 3172.
- [36]. Y. Wang, N. Herron, *J. Phys. Chem.* 95 (1991) 525.
- [37]. R. Wahab, S.G. Ansari, Y.S. Kim, H.K. Seo, H.S. Shin, *Appl. Surf. Sci.* 253 (2007) 7622.
- [38]. A. Umar, Y.B. Hahn, *Nanotechnology* 17 (2006) 2174.
- [39]. D. Ying, Y. Zhang, Y.D. Bai, Z.L. Wang, *Chem. Phys. Lett.* 375 (2003) 96.
- [40]. H. Scholzelt, *Glass: nature, structure and properties*, New York, Springer (1991).
- [41]. G. Exarhos, W. Risen, *Solid State Commun.* 11 (1972) 755.
- [42]. L. Bih, L. Abbas, S. Mohdachi, A. Nadiri, *J. Mol. Struct.* 891 (2008) 173.
- [43]. M.S. Gaffar, Y.B. Saddeek, L. Abd El-Latif, *J. Phys. Chem. Solids* 70 (2009) 173.

P.N.V.V.L. Pramila Rani. "Synthesis, Structural and spectral investigations of Co<sup>2+</sup> doped Cadmiumborate nanocomposite." *IOSR Journal of Engineering (IOSRJEN)*, vol. 08, no. 12, 2018, pp. 17-24.